Pontecorvo reactions in antiproton annihilation at rest in deuterium to $\pi^0 n$, $\pi^0\Delta^0$, ηn, and $\eta\Delta^0$

M. Chiba,[5] T. Fujitani,[4] J. Iwahori,[1,*] M. Kawaguti,[1,†] M. Kobayashi,[2] S. Kurokawa,[2] Y. Nagashima,[4] T. Omori,[4,‡] S. Sugimoto[4,§] M. Takasaki,[2] F. Takeutchi,[3] Y. Yamaguchi,[4] and H. Yoshida[1,‖]
(Fukui-KEK-Kyoto Sangyo-Osaka-Tokyo Metropolitan Collaboration)
[1]*Faculty of Engineering, Fukui University, Fukui, Fukui, 910 Japan*
[2]*KEK, National Laboratory for High Energy Physics, Tsukuba, 305 Japan*
[3]*Faculty of Science, Kyoto Sangyo University, Kita, Kyoto, 603 Japan*
[4]*Department of Physics, Osaka University, Toyonaka, Osaka, 560 Japan*
[5]*Department of Physics, Tokyo Metropolitan University, Hachioji, 192-03, Japan*
(Received 30 September 1996)

Using modularized NaI(Tl) detectors, we carried out a high statistics measurement of inclusive γ-ray, π^0, and η spectra, and determined the branching ratios or upper limits of Pontecorvo reactions $\overline{pd}\to\pi^0 n$, $\pi^0\Delta^0$, ηn, and $\eta\Delta^0$ from the corresponding monochromatic peaks in them. The obtained branching ratios are $B(\overline{pd}\to\pi^0 n)=(1.03\pm0.41)\times10^{-5}$, $B(\overline{pd}\to\pi^0\Delta^0)=(4.67\pm1.66)\times10^{-5}$, $B(\overline{pd}\to\eta n)<8.94\times10^{-6}$ (95% C.L.), and $B(\overline{pd}\to\eta\Delta^0)<6.49\times10^{-5}$ (95% C.L.). [S0556-2821(97)04305-1]

PACS number(s): 13.75.Cs, 25.10.+s

I. INTRODUCTION

At least two mesons are produced in the annihilation of an antiproton with a single nucleon into hadrons. In the annihilation of an antiproton with deuterium, however, reactions associated with only one meson in the final state are possible. Pontecorvo [1] studied the possibility of such unusual processes which are allowed only on bound nucleons. The so-called Pontecorvo reactions mentioned above have mostly been treated theoretically in two-step processes (Fig. 1), for example, $\overline{pd}\to\pi MN'\to\pi N$ with M a meson in the intermediate state such as π, ρ, etc., and $N(N')$ a nucleon. The primary interest in the Pontecorvo reactions is whether they can be explained in two-step processes. If the explanation by two-step processes fails or is insufficient, the question is whether the Pontecorvo reactions are dominated by two-step processes or by some other (more interesting) processes due to the formation of the quark-gluon plasma [2], etc. In case the two step processes can explain the experimental result, one can still probe the deuterium wave function. The branching ratios of Pontecorvo reactions should be sensitive to the deuterium wave function at small internucleon distances, i.e., the high momentum components, where non-nucleonic degrees of freedom may play an important role. They should also be sensitive to the behavior of the meson-nucleon form factors, as the momentum transfer at the MNN' vertex is large. A short review on the Pontecorvo reactions can be seen in Ref. [3].

Experimental data [4–7] on the Pontecorvo reactions are scarce except for the reaction $\overline{pd}\to\pi^- p$, which has also been studied theoretically [8–15]. The experimental values reported for the branching ratio $B(\overline{pd}\to\pi^- p)$ are in the order of 10^{-5}; $(0.9\pm0.4)\times10^{-5}$in a bubble chamber experiment [4], $(2.8\pm0.3)\times10^{-5}$ in PS183 experiment (at LEAR) [5], $(1.4\pm0.7)\times10^{-5}$ in the ASTERIX experiment [6] and $(1.2\pm0.14)\times10^{-5}$ in OBELIX experiment [7]. A preliminary result [8] of $B(\overline{pd}\to\pi^- p)=(1.46\pm0.13)\times10^{-5}$ has been deduced from the Crystal Barrel experiment on $\overline{pd}\to\pi^0 n$ assuming the isospin invariance. The result of calculations in two-step models strongly depends [9–11] on the choice of deuterium wave functions (Hulthen, Paris, Bonn, etc.) as well as on the meson-nucleon form factors (monopole or dipole type, cutoff parameter Λ^2). Typical values obtained for $B(\overline{pd}\to\pi^- p)$ are 2.7×10^{-6} [9], 3.8×10^{-5} [10], and 8.5×10^{-6} [11]. Since calculations based upon the two-step approaches usually give smaller values [12] than the experimental ones, alternative approaches [3] have also been elaborated, including a statistical model of evaporation of a fireball [13], a Reggeon diagram technique [14], a relativistic two-step model [15], etc. Interest in other channels than $\overline{pd}\to\pi^- p$ is discussed in [3,14]. A preliminary result

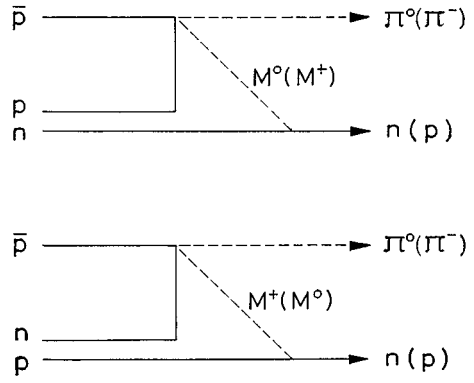

FIG. 1. Two-step processes for the Pontecorvo reaction $\overline{pd}\to\pi^0 n$ or $\pi^- p$ with $M=\pi$, ρ, etc.

*Present address: Kochi Medical School, Nankoku, 783 Japan.
†Deceased.
‡Present address: KEK, National Laboratory for High Energy Physics, Tsukuba, 305 Japan.
§Present address: Institute for Nuclear Study, Univ. of Tokyo, Tanashi, 188 Japan.
‖Present address: Naruto University of Education, Naruto, 772 Japan.

on some other channels ($\overline{pd}\to\eta n$, ωn, $\eta' n$) have also been reported in [8].

We have carried out an experiment on $\overline{pp}$[16–18] and $\overline{pd}$ [19] annihilations at rest with the main aims of searching for baryonia below the NN threshold and measuring the branching ratios of $\overline{pp}$ and $\overline{pn}$ annihilations into different two meson channels. In the above experiment with a deuterium target, we have carried out a high statistics measurement of inclusive γ-ray, π^0, and η meson spectra. The reactions $\overline{pd}\to\pi^0 n$ and ηn should show up as a monochromatic peak in the π^0 spectra at an energy of $E(\pi^0)=1253$ MeV and in the η spectra at $E(\eta)=1304$ MeV, respectively. The reactions $\overline{pd}\to\pi^0\Delta^0(1232)$and $\eta\Delta^0$, which are expected at $E(\pi^0)=1141$ MeV and $E(\eta)=1191$ MeV, respectively, can also be assessed in the present experiment. Since some amount of high energy π^0 were registered as single γ rays due to the limited modularity of the γ-ray detectors, the reactions $\overline{pd}\to\pi^0 n$ and $\pi^0\Delta^0$ should show up as monochromatic peaks also in the inclusive γ-ray spectra. We therefore estimated the yields (i.e., branching ratios) or the upper limits of $\overline{pd}\to\pi^0 n$ and $\pi^0\Delta^0$ from the inclusive π^0 and γ-ray spectra, and of $\overline{pd}\to\eta n$ and $\eta\Delta^0$ from the inclusive η spectra. It is the aim of the present paper to describe the result of the above-mentioned measurement.

II. EXPERIMENT AND DATA REDUCTION

The experimental setup was described in [16,19]. A secondary $\overline{p}$ beam at 580 MeV/c from the KEK 12 GeV proton synchrotron (PS) was made to stop inside a liquid D_2 target of 14 cm (in diameter) $\times$ 23 cm (length). The emitted γ rays were measured with a modularized NaI(Tl) calorimeter assembled into a half barrel covering an effective acceptance of 22% of 4π sr. Charged particles were tracked with cylindrical as well as flat multiwire proportional chambers (MWPC's) covering 93% of 4π sr.

We obtained 1.92×10^7 event in total under the triggering condition of (i) ''stopping antiproton'' = a slow antiproton being incident on the liquid D_2 cell and (ii) ''clustering logic'' = one or two γ rays falling on the NaI.

The instrumental energy resolution for $\pi^0\to\gamma\gamma$ ($\eta\to\gamma\gamma$) should be better than that [16] of single γ rays having the same energy as $\pi^0(\eta)$, since the energy resolution $\Delta E/E$ of each γ ray is approximately proportional to $E^{-0.25}$ for the present detector. The energy resolution depends on the energy partition into γ rays, but is better by a factor of 0.89 in average. For the Pontecorvo reactions on deuterium, it is not necessary to take into account the Doppler smearing [19] of γ-ray energies, which has to be taken into account for reactions on single nucleons in deuterium. Consequently, the full width at half-maximum (FWHM) energy resolution of the $\pi^0(\eta)$ energy E was taken as

$$\Delta E/E=0.055/[E\ \ (\text{in GeV})]^{1/4} \tag{1}$$

by multiplying the energy resolution $0.062/[E\ \ (\text{in GeV})]^{1/4}$ [16] for γ rays with the above mentioned factor (0.89). The instrumental energy resolution for $\pi^0\to2\gamma\to1\gamma$ (mistaken) was also taken to be the same as above.

The saturation of each module, typically 5% at 650 MeV, was taken into account using data of the excitation curve obtained for an electron beam [16] at 200, 400, 650, and 900 MeV. Overall energy scale was determined to within 2% using 129 MeV γ rays produced in $\pi^- p\to\pi^0 n$ and 750 MeV π^0 mesons in $\overline{pp}\to\pi^0\rho^0/\pi^0\omega$. With the above calibration, the π^0 peak due to $\overline{pd}\to\pi^0\pi^- p_s$ was clearly observed near the right position of 938 MeV [20]. For the present measurement of Pontecorvo reactions, the maximum energies of interest (1253 MeV for π^0 and 1304 MeV for η) are substantially higher than 938 MeV. However, the energy deposited in a single NaI module is mostly well below half of the π^0 or η energies due to the minimum opening angles of two γ rays (discussed later) and the configuration of the calorimeter [16]. Consequently, the maximum energy deposited in a single module is less than 700 MeV, i.e., well within the range where the gain calibration as well as the correction for the saturation effect is precise for each NaI module. The accuracy of the energy scale within $\pm2\%$ is expected to be valid at least up to the π^0 energy of 1253 MeV for $\overline{pd}\to\pi^0 n$ (1304 MeV for $\overline{pd}\to\eta n$) since the energy registered in each module is mostly much less than 938 MeV.

A. $\overline{pd}\to\pi^0 n$ and $\pi^0\Delta^0(1232)$ from π^0 spectra

In the data analysis, we first removed those events which have hardware errors in readout or ambiguous tracks of the incoming slow antiproton. The vertex was then determined using the tracks of the antiproton and the outgoing charged particles. For all-neutral events, the vertex was determined from the track of the antiproton and its range estimated from the energy loss in the 3-mm thick Si solid state detector (SSD) [21], which was mounted just downstream of the beam degrader. Requiring that (i) the vertex should not be located outside the target cell by more than 2 cm radially and 1.5 cm longitudinally and (ii) the rms distance from the vertex to the charged tracks should be less than 3 cm, we obtained $N_v=6.93\times10^7$ events with two ore more γ rays hitting the NaI detector. The $\gamma\gamma$ invariant mass $M(\gamma\gamma)$ was calculated [17] for any combinations of the γ rays. The $M(\gamma\gamma)$ spectra for 60% of the total statistics are given in Figs. 2(a) and 2(b) for two cases of the energy sum of two γ rays larger than 825 and 1035 MeV, respectively. For the former case [Fig. 2(a)], both π^0 and η peaks are clearly seen, showing that the calculation of the invariant mass, including the energy calibration, is good even for pairs of γ rays whose energy sum is large. For the latter case [Fig. 2(b)], however, no clear peaks are seen; the absence can be explained by the fact that the energy threshold of 1035 MeV is above the kinematical limit of π^0 or η energy in usual annihilation processes of $\overline{pp}$ or $\overline{pn}$. The π^0's and η's in this high-energy region are mostly fake; they must be due to accidental combination of two γ rays coming from different π^0's. We selected π^0's by applying an invariant mass cut of ±31 MeV/c^2, which corresponds to about $\pm1.8\sigma$ if $\sigma\sim17.6$ MeV/$c^2$is taken from the energy range above 825 MeV [see Fig. 2(a)]. The above value of σ is larger than 14 MeV/c^2 [20] which was obtained for all π^0's with any energies; most of π^0's have much lower energies than 825 MeV. The degradation of the invariant mass resolution for high energy π^0's is qualitatively explicable in terms of small

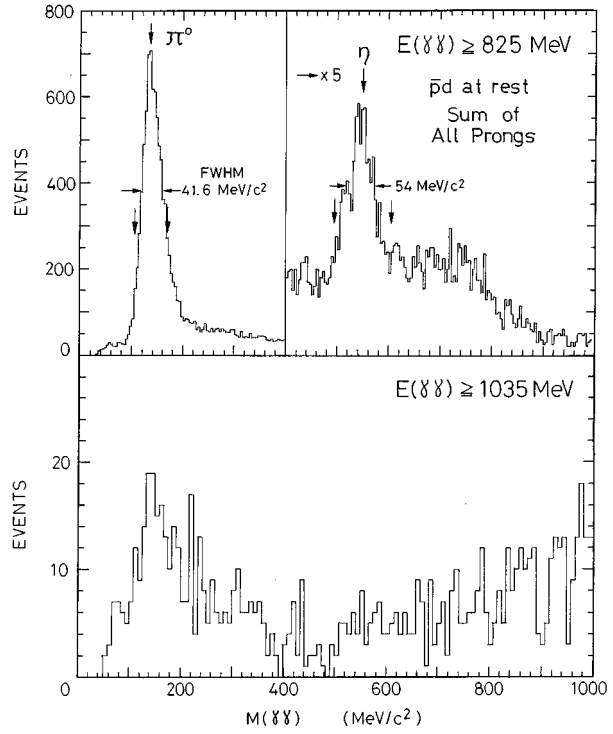

FIG. 2. The $\gamma\gamma$ invariant mass spectra for two γ rays with the total energy larger than (a) 825 MeV and (b) 1035 MeV. Only 60% of the total statistics is included in the figure.

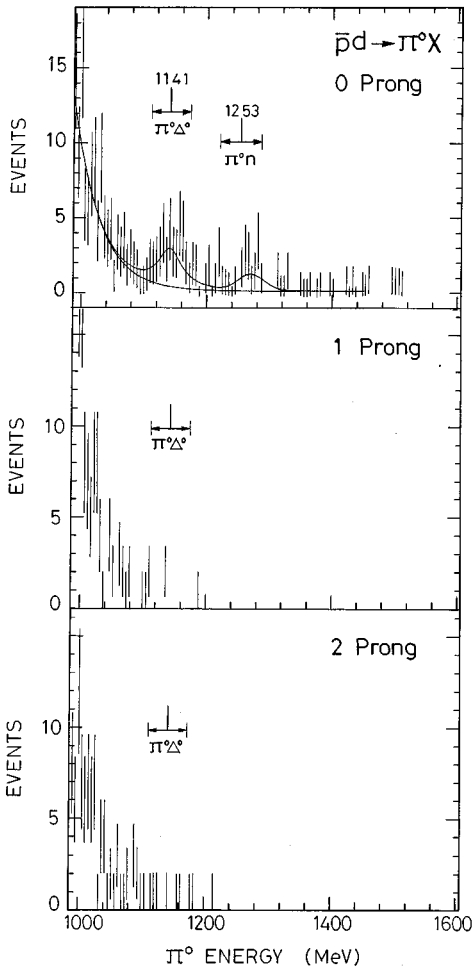

FIG. 3. Inclusive π^0 spectra from $\overline{pd}$ annihilation at rest. The 0-pronged spectrum is given in the fractional binning (see the text). A solid curve gives the fit (see Table I for the fit and the text for χ^2/N_{DF}). The horizontal arrows at the $\pi^0 n$ and $\pi^0\Delta^0$ positions show the instrumental widths (see the text) of ± 32.6 MeV in $\pm$FWHM/2 and ± 30.8 MeV in $\pm\Gamma/2$, respectively.

$(\gamma\gamma)$ opening angles at high energies. The obtained π^0 spectra above 1000 MeV are presented in Fig. 3 separately for the charge multiplicity of 0, 1, and 2. The π^0 spectra below 1000 MeV will be given elsewhere [20]. The peaks due to the reactions $\overline{pd}\rightarrow\pi^0 n$ and $\pi^0\Delta^0$ are expected to appear at 1253 and 1141 MeV with a width (in FWHM) $=65.1$ MeV [from Eq. (1)] and $\Gamma=61.6$ MeV (see below), respectively. The minimum opening angle of two γ rays from π^0 is 12.4° (13.6°) at 1253 MeV (1141 MeV).

The Breit-Wigner width for the final states involving Δ^0 (1232) was determined in the following way; if one ignores the instrumental resolution, the π^0 energy spectrum for the reaction $\overline{pd}\rightarrow\pi^0\Delta^0$ has a Breit-Wigner shape of

$$1/[(E-E_0)^2+(\Gamma_0/2)^2], \tag{2}$$

where E_0 is the center energy (1141 MeV) and $\Gamma_0 = \Gamma(\Delta^0)M(\Delta^0)/(M_{\bar{p}}+M_d)=50.4$ MeV with Γ (Δ^0), $M(\Delta^0)$, $M_{\bar{p}}$ and M_d the full width (115 MeV) of $\Delta^0(1232)$, mass of Δ^0, masses of (anti)proton and deuterium, respectively. The instrumental resolution of π^0 energy was then taken into account by numerically folding the above Breit-Wigner shape with it. The folded shape was approximated again by another Breit-Wigner shape similar to Eq. (2) with Γ_0 replaced by Γ. The Γ was found to be 61.6 MeV.

B. $\overline{pd}\rightarrow\eta n$ and $\eta\Delta^0$ (1232) from η spectra

The constraints on the vertex reconstruction were the same as for the π^0 spectra. η's were selected with an invariant mass cut of ± 57 MeV/c^2 which corresponds to about $\pm 2.5\sigma$ with $\sigma=23$ MeV/c^2 [see Fig. 2(a)]. The above value of σ for high energy η's ($\geq$825 MeV) is smaller than that (25 MeV/c^2) obtained with all η's included. This tendency is contrary to the case of π^0's. When the energy increases, there must be two effects on the $\gamma\gamma$ invariant mass resolution; one is an improving effect due to an improvement of each γ-ray energy resolution, and the other a degrading effect due to decreasing opening angles of two γ rays. The observed improvement is explicable in terms of dominance of the former effect. The degrading effect will be small since the opening angle is always much larger than the minimum separation angle which is 10° with the present detector [15]. The obtained η spectra above 1000 MeV are presented in Fig. 4 separately for the charge multiplicity of 0, 1, and 2. Most of η's have energies below 1000 MeV; the η spectra below 1000 MeV will be given elsewhere [20]. The peaks due to the reactions $\overline{pd}\rightarrow\eta n$ and $\eta\Delta^0$ are expected to appear at 1304 and 1191 MeV with a Gaussian width (in FWHM) of 67.1 MeV [from Eq. (1)] and Γ of 61.6 MeV, respectively. The Γ for $\overline{pd}\rightarrow\eta\Delta^0$ is almost the same in magnitude as for $\overline{pd}\rightarrow\pi^0\Delta^0$(see Sec. II A). The minimum opening angle of two γ rays from η is 49.8° (54.9°) at 1304 MeV (1191 MeV).

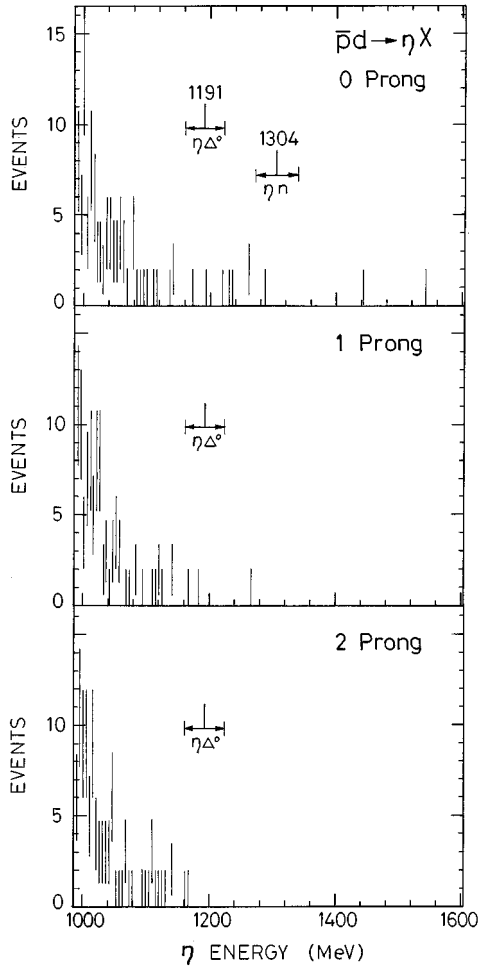

FIG. 4. Inclusive η spectra from $\overline{\text{pd}}$ annihilation at rest. The horizontal arrows at the ηn and $\eta\Delta^0$ positions show the instrumental widths (see the text) of ± 33.6 MeV in $\pm$FWHM/2 and ± 30.8 MeV in $\pm\Gamma/2$, respectively.

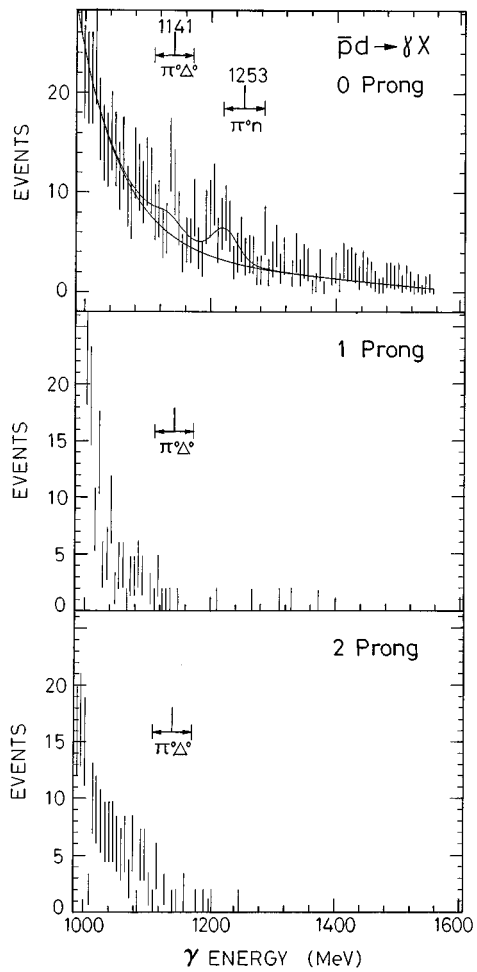

FIG. 5. Inclusive γ-ray spectra from $\overline{pd}$ annihilation at rest. The 0-pronged spectrum is given in the fractional binning (see the text). A solid curve gives the fit (see Table I for the fit and the text for χ^2/N_{DF}). The horizontal arrows at the $\pi^0 n$ and $\pi^0\Delta^0$ positions show the instrumental widths (see the text) of ± 32.6 MeV in $\pm$FWHM/2 and ± 30.8 Mev in $\pm\Gamma/2$, respectively.

C. $\overline{pd} \to \pi^0 n$ and $\pi^0\Delta^0$ (1232) from γ-ray spectra

The same constraints as for the π^0 spectra were adopted in the vertex reconstruction. The statistics of the incident antiprotons for the γ-ray spectra was about 6% higher than for the π^0 and η spectra, due to an accidental loss of some data tapes for the latter. We obtained $N_v = 7.32 \times 10^6$ events and $N\gamma = 6.70 \times 10^6$ γ rays above 10 MeV. The obtained inclusive γ-ray spectra below 1000 MeV are given in [19] separately for each charge multiplicity as well as for their sum. For the Pontecorvo reactions, however, the relevant energy is much higher. The γ-ray spectra above 1000 MeV are given in Fig. 5 separately for the charge multiplicity of 0, 1, and 2. The expected positions and the widths of the monochromatic peaks should be the same as in the π^0 spectra described in Sec. II A.

III. RESULTS

The branching ratio $B(\overline{pd} \to MN)$ of the reaction $\overline{pd} \to MN$ with $M = \pi^0$ or η and $N = n$ or Δ^0 satisfies the following relation:

$$N_{\bar{p}} \varepsilon B(\overline{pd} \to MN) = A, \tag{3}$$

where A is the area (total number of events) of the monochromatic π^0 or η peak (above the background) due to the assumed reaction, $N_{\bar{p}}$ the number of stopped antiprotons and ε the overall detection efficiency.

We estimated $N_{\bar{p}}$ in two different ways [17,20] (i) dividing the total π^0 (or γ-ray) intensity by the detection efficiency and (ii) dividing the number of events after vertex reconstruction (N_v) by the efficiency of the cluster logics (one or two γ rays falling on the NaI). The efficiencies were obtained by a Monte Carlo calculation. Both methods gave consistently $N_{\bar{p}} = 1.25 \times 10^7$ and 1.32×10^7 antiprotons for the final states with the charge multiplicity $N_{ch} \geq 1$ for π^0 (or η) and γ rays, respectively, within an ambiguity of 5%. The $N_{\bar{p}}$ for $N_{ch} = 0$ was taken to be larger than the above by 31% due to the looser vertex cut, as already described in Sec. II A.

The efficiency ε is given as a product of the following four factors:

(i) ε_g = geometrical acceptance for the detection of π^0 (or η) $\to \gamma\gamma$. Loss of γ rays due to $\gamma \to e^+e^-$ conversion (6% per γ ray) in target and vacuum chamber walls is taken into account. It was obtained by a Monte Carlo calculation and is given in Fig. 6.

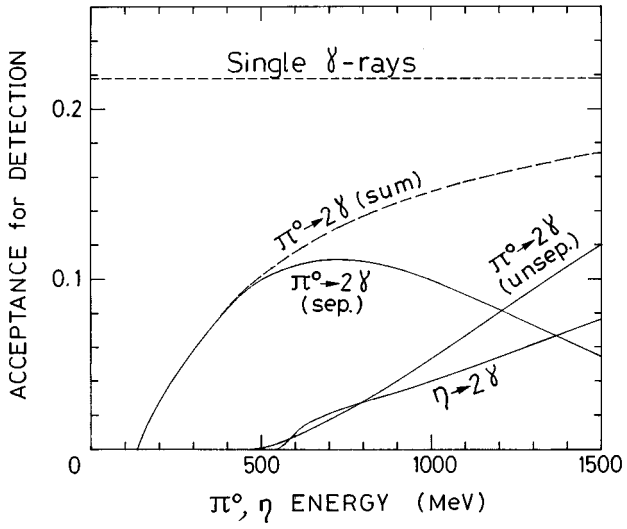

FIG. 6. Geometrical acceptances (ε_g) of the NaI:Tl detector for detecting $\pi^0\to\gamma\gamma$ separately, mistaking them for a single γ ray, and detecting $\eta\to\gamma\gamma$ separately. The acceptance for single γ rays is also shown by a dotted curve. Loss of γ rays due to $\gamma\to e^+e^-$ conversion (6% per γ ray) in target and vacuum chamber walls is taken into account. Invariant-mass cut for $\pi^0(\eta)\to\gamma\gamma$ is not included.

(ii) ε_1=efficiency of invariant mass cut for π^0 (η)=0.93 (0.98) for the cut at $\pm1.8\sigma$ ($\pm2.5\sigma$).

(iii) ε_{ov}=0.90 due to the decrease in the detection efficiency caused by the existence of additional charged particles (for $\Delta^0\to\pi^-p$) or $\pi^0\to\gamma\gamma$ (for $\Delta^0\to\pi^0n$) overlapping the monochromatic π^0 or η. It was estimated by a Monte Carlo calculation for the final states involving Δ^0.

(iv) ε_{br}=branching ratios $B(\Delta^0\to$one- or two-pronged state)=0.41, $B(\Delta^0\to$0-pronged state)=0.59 and $B(\eta\to\gamma\gamma)$=0.39. The former two values are obtained by correcting the branching ratios $B(\Delta^0\to\pi^-p)$=0.33, $B(\Delta^0\to\pi^0n)$=0.67 for $\gamma\to e^+e^-$ conversion (6% per γ ray) before entering the NaI calorimeter. Registration of $\Delta^0\to\pi^-p$ into 0-pronged spectra due to an inefficiency of charged particle tracking (7% per charge) is negligibly small.

The values of ε are listed in Table I. Its overall ambiguity is about 10% of ε.

To obtain the area A, the π^0 of η spectrum was fitted with a narrow Gaussian shape (or a Breit-Wigner shape for the case of recoil Δ instead of neutron) centered at about the expected energy superimposed to a background of $a+b\exp(cE)$, where a, b, and c are constants and E is the energy. For γ rays, the constant term (a) in the background was changed to a linear function of energy to get a good fit.

The scattering from bin to bin in the spectra is not small due to the low statistics. The scattering is not a serious problem to obtain the upper limits of the yields. For the 0-pronged spectra of π^0 and γ rays, however, we determined finite yields by fitting. To improve the stability of the fit for different choice of the bin width, fitting region and function, etc., we adopted the fractional binning. For any event with an energy E between two bin centers E_k and E_{k+1}, the event was registered to both bins by an amount $(E_{k+1}-E)/\delta$ and $(E-E_k)/\delta$, respectively, where δ denotes the bin width. The 0-pronged π^0 and γ-ray spectra are given in Figs. 3 and 5, respectively, in the fractional binning. From comparison between the fractional and ordinary binnings for a simplest example of uniform random distribution of events in a certain energy range, we can see that the χ^2 of the fit in the

TABLE I. Obtained result on Pontecorvo reactions. Area (A) gives the number of events in the peak obtained by fitting. For σ (the rms error of A), see the text. When fitting does not give any clear peaks, $N_{\rm bg}$(see the text) is given instead of A. The last column gives the fitted energy and the width of the π^0 or η peak in MeV.

Reaction (N_{ch}) $\overline{p}d\to MN$	Stopped $\overline{p}$ $N_{\overline{p}}$	Efficency (ε) ($\varepsilon_g,\varepsilon_1,\varepsilon_{ov},\varepsilon_{br}$)	Area (A)$\pm\sigma(A)$ or $N_{\rm bg}$	Branching ratio $B(\overline{p}d\to MN)$	Energy (width)
$\overline{p}d\to\pi^0n$ (N_{ch}=0) ($\pi^0\to2\gamma$)	1.64×10^7	(0.076,0.93,...,...)	10.1±5.4	$(8.71\pm4.66)\times10^{-6}$	1269.3±9.8 (σ=18.9±5.9)
" "(N_{ch}=0) ($\pi^0\to2\gamma\to1\gamma$ mistaken)	1.73×10^7	(0.088,...,...,...)	23.6±13.0	$(1.55\pm0.86)\times10^{-5}$	1221.8±6.7 (σ=19.5±7.4)
$\overline{p}d\to\pi^0\Delta^0$ (N_{ch}=0) ($\pi^0\to2\gamma$, $\Delta^0\to\pi^0n$)	1.64×10^7	(0.088,0.93,0.9,0.59)	33.3±11.8	$(4.67\pm1.66)\times10^{-5}$	1141.5±9.5 ($\Gamma/2$=21.6±6.2)
" "(N_{ch}=1,2) ($\pi^0\to2\gamma$, $\Delta^0\to\pi^-p$)	1.25×10^7	(0.088,0.93,0.9,0.41)	$N_{\rm bg}$=9	$<7.37\times10^{-5}$ (95% C.L.)	
" "(N_{ch}=0) ($\pi^0\to2\gamma\to1\gamma$ mistaken, $\Delta^0\to\pi^0n$)	1.73×10^7	(0.072,...,0.9,0.59)	32.3±18.2	$<9.39\times10^{-5}$ (95% C.L.)	1132.6±24.2 [$\Gamma/2$=30.8 (fix)]
" "(N_{ch}=1,2) ($\pi^0\to2\gamma\to1\gamma$ mistaken, $\Delta^0\to\pi^-p$)	1.32×10^7	(0.072,...,0.9,0.41)	$N_{\rm bg}$=19	$<1.49\times10^{-4}$ (95% C.L.)	
$\overline{p}d\to\eta n$ (N_{ch}=0) ($\eta\to2\gamma$)	1.64×10^7	(0.062,0.98,...,0.39)	$N_{\rm bg}$=1	$<8.94\times10^{-6}$ (95% C.L.)	
$\overline{p}d\to\eta\Delta^0$ (N_{ch}=0) ($\eta\to2\gamma$, $\Delta^0\to\pi^0n$)	1.64×10^7	(0.054,0.98,0.9,0.230)	$N_{\rm bg}$=3	$<6.49\times10^{-5}$ (95% C.L.)	
" "(N_{ch}=1,2) ($\eta\to2\gamma$, $\Delta^0\to\pi^-p$)	1.25×10^7	(0.054,0.98,0.9,0.160)	$N_{\rm bg}$=4	$<1.53\times10^{-4}$ (95% C.L.)	

fractional binning is $\frac{2}{3}$ times that in the ordinary binning. The center values and the standard deviations of the fitting variables are essentially unchanged when the statistics is large. We used the above conversion for the present analysis while the statistics was not large enough.

We searched for narrow monochromatic peaks with a width between 0.7 and 1.0 times the instrumental one (or the Breit-Wigner width corrected for the instrumental width). A peak with the statistical significance as large as or larger than 2σ was obtained for $\pi^0 n$ and $\pi^0\Delta^0$ in the 0-pronged π^0 spectrum (Fig. 3) and γ-ray spectrum (Fig. 5). The solid curves give the obtained fit. For the 0-pronged spectrum of π^0 (γ rays), $\chi^2/N_{\rm DF}$ (degree of freedom) was $\frac{62}{75}$ ($\frac{77}{80}$) when converted into ordinary binning according to the discussion given in the previous paragraph. The peak area A obtained by the fit is given in Table I together with its rms error $\sigma(A)$. The $\sigma(A)$ was taken to be the larger one of the fitting error given by the minimization routine MINUIT [22] or the rms fluctuation of the background events. The latter can be written as $(N_{\rm bg})^{1/2}/\kappa$, where $N_{\rm bg}$ is the total number of events lying within the FWHM of the Gaussian peak (or Γ for the Breit-Wigner peak). The $\kappa=0.76$ (0.5) is the area factor, i.e., the fraction of the Gaussian (Breit-Wigner) peak lying within the FWHM (Γ). $N_{\rm bg}$ was calculated assuming the instrumental FWHM or Γ. We adopted the above definition of $\sigma(A)$ since the MINUIT error varied sizably depending on the fitting condition due to the low statistics. Both errors, $(N_{\rm bg})^{1/2}/\kappa$ and the MINUIT error, however, were roughly similar in magnitude to each other.

For the other final states, no narrow peaks were obtained with the statistical significance above 2σ. So, only the upper limit was estimated. If the copious background exists in the peak area, the upper limit of the peak area can be given as

$$A<1.64(N_{\rm bg})^{1/2}/\kappa \quad (95\% \ \text{C.L.}). \tag{4}$$

However, for all the final states under consideration, the intensity in the peak is so small and the tail of the background spectrum already falls to a level low enough at a little lower energy than the peak position (see Figs. 3–5). So, we cannot exclude the possibility that the intensity in the peak is not dominated by background but by true events. Consequently, we took for safety, instead of Eq. (4),

$$A<[N_{\rm bg}+1.64(N_{\rm bg})^{1/2}]/\kappa \quad (95\% \ \text{C.L.}), \tag{5}$$

and give the $N_{\rm bg}$ in Table I instead of A.

The branching ratios or the upper limits (95% C.L.) calculated according to Eq. (3) are given in Table I. Branching ratios $B(\overline{pd}\to\pi^0 n)=(8.71\pm4.66)\times10^{-6}$ and $B(\overline{pd}\to\pi^0\Delta^0)=(4.67\pm1.66)\times10^{-5}$ were derived from the 0-pronged π^0 spectrum. The upper limit of the latter quantity derived from the one- or two-pronged π^0 spectrum is consistent with the obtained finite value. The 0-pronged γ-ray spectrum includes a larger background than the π^0 spectrum. A peak is seen for $\overline{pd}\to\pi^0 n$ with the statistical significance as large as 2σ. By combining both results from the π^0 and the γ-ray spectra, we obtained $B(\overline{pd}\to\pi^0 n)=(1.03\pm0.41)\times10^{-5}$. Although there is a small peak in the 0-pronged γ-ray spectrum corresponding to $\overline{pd}\to\pi^0\Delta^0$, the statistical significance is less than 2σ and the fit significantly depended on the fitting conditions. The width is visibly too narrow compared with the prediction. Consequently, only the upper limit was derived (see Table I). The upper limits for $B(\overline{pd}\to\pi^0\Delta^0)$ derived from the γ-ray spectra are consistent with the finite value obtained from the 0-pronged π^0 spectrum. For $B(\overline{pd}\to\eta n)$ and $B(\overline{pd}\to\eta\Delta^0)$, only the upper limits were derived from the η spectra.

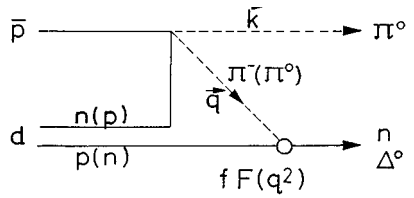

FIG. 7. Kinematical quantities used in the discussions of $\overline{pd}\to\pi^0 n$ and $\pi^0\Delta^0$.

IV. SUMMARY AND DISCUSSIONS

Summarizing the above we obtained the following branching ratios or upper limits:

$$\begin{aligned} B(\overline{pd}\to\pi^0 n)&=(1.03\pm0.41)\times10^{-5},\\ B(\overline{pd}\to\pi^0\Delta^0)&=(4.67\pm1.66)\times10^{-5},\\ B(\overline{pd}\to\eta n)&<8.94\times10^{-6} \quad (95\% \ \text{C.L.}),\\ B(\overline{pd}\to\eta\Delta^0)&<6.49\times10^{-5} \quad (95\% \ \text{C.L.}). \end{aligned} \tag{6}$$

The obtained yield for the first reaction $\overline{pd}\to\pi^0 n$ should be compared with the half of $B(\overline{pd}\to\pi^- p)$ mentioned in Sec. I. The present result is consistent with all the four results [4–7] and also the preliminary one given in [8]. The obtained upper limit on $B(\overline{pd}\to\eta n)$ is consistent with the preliminary result of $B(\overline{pd}\to\eta n)=(2.91\pm0.44)\times10^{-6}$ obtained at LEAR by Amsler *et al.* [8]. To the authors' knowledge, neither experimental results nor predictions are found in publications on the other two reactions $\overline{pd}\to\pi^0\Delta^0$ and $\eta\Delta^0$.

We will discuss below the $\pi^0\Delta^0/\pi^0 n$ ratio $=B(\overline{pd}\to\pi^0\Delta^0)/B(\overline{pd}\to\pi^0 n)$ under the assumption of two step processes. If the experimental value cannot be explained, it may suggest existence of more interesting processes related to, for instance, quark-gluon plasma. We consider the differences in the available phase space, the isospin coefficients and the vertex factor, by assuming the magnitude of the dynamical part the same. The phase space is proportional [23] to the final state momentum q in the c.m. system (c.m.s.). Its contribution to the above ratio is given by 1132.5 (MeV/c)/1246.0 (MeV/c)=0.9089. The contribution of the isospin part to the above ratio is unity, since the amount of $I=1/2$ (initial state) is the same for both final states. Referring to Fig. 7, the vertex factor has a form of $f_{\pi NN}{}^2[(\Lambda^2-m_\pi{}^2)/(\Lambda^2-q^2)]^{2n}$ at the πNN vertex in $\overline{pd}\to\pi^0 n$ and $f^2_{\pi N\Delta}[(\Lambda^{*2}-m_\pi{}^2)/(\Lambda^{*2}-q^2)]^{2n}$ at the $\pi N\Delta$ vertex in $\overline{pd}\to\pi^0\Delta^0$, respectively. The coupling constants $f_{\pi NN}$ and $f_{\pi N\Delta}$ were taken as [24]

$$f_{\pi NN}{}^2/4\pi=0.08 \ \text{ and } \ f^2_{\pi N\Delta}/4\pi=0.37. \tag{7}$$

We follow the conventional choice of monopole form factor ($n=1$) with the cutoff parameters Λ and $\Lambda^*\sim1$ GeV/c ac-

cording to [24]. The four momentum squared q^2 of the pion (see Fig. 7) is not unique in general. In the two step model, however, the initial-state nucleon at the vertex can be approximately taken as on-mass and at rest, giving $\mathbf{k}+\mathbf{q}=0$ in Fig. 7. Then we have

$$q^2 = m_n{}^2 + m_N{}^2 - 2m_N E_n = -1.1674 \ \text{GeV}^2 \quad \text{for} \quad \pi^0 n,$$

and

$$q^2 = m_\Delta{}^2 + m_N{}^2 - 2m_N E_\Delta = -0.7431 \ \text{GeV}^2 \quad \text{for} \quad \pi^0 \Delta^0,$$

where E_n and E_Δ are the energies of the final state baryon n and Δ^0, respectively. Using the above numbers, the contribution of the vertex factor to the $\pi^0\Delta^0/\pi^0 n$ ratios becomes $(0.37/0.08)(0.5629/0.4527)^2 = 7.151$. Multiplying the above three contributions, we obtain 6.50 for $B(\overline{pd} \rightarrow \pi^0\Delta^0)/B(\overline{pd} \rightarrow \pi^0 n)$. The above number can roughly explain the obtained ratio of $(4.67 \pm 1.66)/(1.03 \pm 0.41) = 4.53 \pm 2.42$ in the present experiment.

ACKNOWLEDGMENTS

The authors are indebted to many people, especially to T. Nishikawa, S. Ozaki, H. Sugawara, H. Hirabayashi, and K. Nakai for supporting the present work, to the staff of the PS, the beam channel, and the experimental facilities for skillful operations, and to the staff of the computer center for help in carrying out the analysis. They are deeply thankful to S. Nozawa (Jyonan Women University), M. Maruyama (Tohoku University), and S. Furui (Teikyo University) for helpful discussions and comments on theoretical aspects.

[1] B. M. Pontecorvo, JETP **3**, 966 (1956).
[2] J. Rafelski, Phys. Lett. **91B**, 281 (1980).
[3] A. M. Rozhdestvensky and M. G. Sapozhnikov, Surv. High Energy Phys. **6**, 115 (1992).
[4] R. Bizzarri *et al.*, Lett. Nuovo Cimento **2**, 431 (1969).
[5] G. A. Smith, in *Proceedings of the Elementary Structure of Matter Workshop*, Les Houches, 1987 (Springer, Berlin, 1988), p. 219.
[6] J. Riedelberger *et al.*, Phys. Rev. C **40**, 2717 (1989).
[7] V. G. Ableev *et al.*, JINR rapid commun. No. 2[59]-93, 1993, p. 75.
[8] Crystal Barrel Collaboration, C. Amsler *et al.*, Phys. At. Nuclei **57**, 1602 (1994).
[9] L. A. Kondratyuk and M. G. Sapoznikov, Phys. Lett. B **220**, 333 (1989).
[10] E. Oset and E. Hernandez, Nucl. Phys. **A494**, 533 (1989).
[11] E. A. Kudryavtsev and V. E. Tarasov, Sov. J. Nucl. Phys. **55**, 538 (1992).
[12] L. A. Kondratyuk and M. G. Sapozhnikov, Few-Body Syst. Suppl. **5**, 201 (1992).
[13] J. Cugnon and J. Vandermeulen, Phys. Rev. C **39**, 181 (1989).
[14] A. B. Kajdalov, Sov. J. Nucl. Phys. **53**, 872 (1991).
[15] C. Guaraldo and L. A. Kondratyuk, Phys. Lett. B **256**, 6 (1991).
[16] M. Chiba *et al.*, Phys. Rev. D **36**, 3321 (1987).
[17] M. Chiba *et al.*, Phys. Lett. B **202**, 447 (1988); Phys. Rev. D **38**, 2021 (1988).
[18] M. Chiba *et al.*, Phys. Rev. D **39**, 3227 (1989).
[19] M. Chiba *et al.*, Phys. Rev. D **44**, 1933 (1991).
[20] M. Chiba *et al.* (unpublished).
[21] M. Chiba *et al.*, Nucl. Instrum. Methods Phys. Res. A **276**, 122 (1989).
[22] F. James and M. Roos, Comput. Phys. Commun. **10**, 343 (1975).
[23] See, for example, L. S. Rodberg and R. M. Thaler, *Introduction to the Quantum Theory of Scattering*, Pure and Applied Physics Series Vol. 26 (Academic, New York, 1967).
[24] E. Oset, H. Toki, and W. Weise, Phys. Rep. **83**, 281 (1982).